# A Preliminary Design for the GMT-Consortium Large Earth Finder (G-CLEF)

Andrew Szentgyorgyi[a], Stuart Barnes[b],Jacob Bean[c], Bruce Bigelow[d], Antonin Bouchez[d], Moo-Young Chun[e], Jeffrey D. Crane[g], Harland Epps[h], Ian Evans[a], Janet Evans[a], Anna Frebel[i], Gabor Furesz[a], Alex Glenday[a], Dani Guzman[j], Tyson Hare[g], Bi-Ho Jang[e], Jeong-Gyun Jang[e], Ueejeong Jeong[e], Andres Jordan[i], Kang-Min Kim[e], Jihun Kim[e], Chih-Hao Li[b], Mercedes Lopez-Morales[a], Kenneth Mc Cracken[a], Brian McLeod[a], Mark Mueller[a], Jakyung Nah[e], Timothy Norton[a], Heeyoung Oh[e,f], Jae Sok Oh[e], Mark Ordway[a], Byeong-Gon Park[e,f], Chan Park[e], Sung-Joon Park[e], David Phillips[a], David Plummer[a], William Podgorski[a], Florian Rodler[a], Andreas Seifahrt[c], Kyung-Mo Tak[e], Alan Uomoto[g], Marcos A. Van Dam[k], Ronald Walsworth[a], Young Sam Yu[e], In-Soo Yuk[e]

[a]Harvard-Smithsonian Center for Astrophysics, 60 Garden St., Cambridge, MA 02140;
[b]Stuart Barnes Optical Design, Sumatrastraat 108a, Amsterdam, The Netherlands
[c]University of Chicago, 640 S. Ellis Ave, Chicago, IL 60637;
[d]Giant Magellan Telescope Organization, 251 South Lake Street, Pasadena, CA 91101
[e]Korea Astronomy and Space Science Institute (KASI) 776 Daedeokdae-ro, Yuseong-gu, Daejeon, 305-348, Republic of Korea
[f]Korea University of Science and Technology, 217 Gajeong-ro, Yuseong-gu, Daejeon 305-350, Republic of Korea
[g]The Observatories of the Carnegie Institution for Science, 813 Santa Barbara St., Pasadena, CA 91101;
[h]UCO/Lick Observatory, University of California, Santa Cruz, CA 95064;
[i]Massachusetts Institute of Technology and Kavli Institute for Astrophysics and Space Research, 77 Massachusetts Ave., Cambridge, MA 02139;
[j]Pontificia Universidad Catolica de Chile, Vicuna Mackenna 4860, Macul, Santiago, Chile;
[k]Flat Wavefronts, PO Box 1060, Christchurch, 8140, New Zealand

## ABSTRACT

The GMT-Consortium Large Earth Finder (G-CLEF) is an optical-band echelle spectrograph that has been selected as the first light instrument for the Giant Magellan Telescope (GMT). G-CLEF is a general-purpose, high dispersion spectrograph that is fiber fed and capable of extremely precise radial velocity measurements. The G-CLEF Concept Design (CoD) was selected in Spring 2013. Since then, G-CLEF has undergone science requirements and instrument requirements reviews and will be the subject of a preliminary design review (PDR) in March 2015. Since CoD review (CoDR), the overall G-CLEF design has evolved significantly as we have optimized the constituent designs of the major subsystems, i.e. the fiber system, the telescope interface, the calibration system and the spectrograph itself. These modifications have been made to enhance G-CLEF's capability to address frontier science problems, as well as to respond to the evolution of the GMT itself and developments in the technical landscape. G-CLEF has been designed by applying rigorous systems engineering methodology to flow Level 1 Scientific Objectives to Level 2 Observational Requirements and thence to Level 3 and Level 4. The rigorous systems approach applied to G-CLEF establishes a well defined science requirements framework for the engineering design. By adopting this formalism, we may flexibly update and analyze the capability of G-CLEF to respond to new scientific discoveries as we move toward first light. G-CLEF will exploit numerous technological advances and features of the GMT itself to deliver an efficient, high performance

Ground-based and Airborne Instrumentation for Astronomy V, edited by
Suzanne K. Ramsay, Ian S. McLean, Hideki Takami, Proc. of SPIE Vol. 9147,
914726 · © 2014 SPIE · CCC code: 0277-786X/14/$18 · doi: 10.1117/12.2056741

instrument, e.g. exploiting the adaptive optics secondary system to increase both throughput and radial velocity measurement precision.

**Keywords:** Echelle spectrograph, precision radial velocity, G-CLEF, GMT, high dispersion spectroscopy, ELTs

## 1. INTRODUCTION

The GMT-Consortium Large Earth Finder (G-CLEF) is an optical-band echelle spectrograph that is in preliminary design phase and will be delivered as the first Giant Magellan Telescope (GMT)[1] science instrument. Preliminary design review (PDR) is scheduled for March 2015 and G-CLEF will commence science operations in mid-2020. The design of G-CLEF has been guided by requirements to enable a broad range of scientific investigations and to exploit the large aperture of the GMT, which may have the largest aperture of any optical-near infrared (NIR) telescope in the world at first light. The conceptual design review (CoDR) design of G-CLEF has been discussed in an earlier publication[2]. Since that time the design has been considerably optimized[3,4] and the requirements have been flowed down from science drivers to Level 4 requirements. A key science driver for G-CLEF is that for radial velocity (RV) precision sufficient to detect the reflex motion induced in a Solar-like star by an Earth-mass planet orbiting in the habitable zone (~10 cm/sec). The spectrograph is fiber fed, deployed at a gravity-invariant location and thermally stabilized to enable precision radial velocity (PRV) measurements. The length of the fiber feed is minimized to extend the blue end of the passband to 3500Å for stellar abundance investigations, especially the characterization of the most metal-poor stars. A particular innovation has been the application of systems engineering formalism to the development of a radial velocity error budget[5]. The context for the G-CLEF science mission within the GMT strategic science plan is discussed elsewhere[6].

Given that the scientific landscape is evolving extremely rapidly, we update several of the science drivers and top-level instrument requirements in this paper.

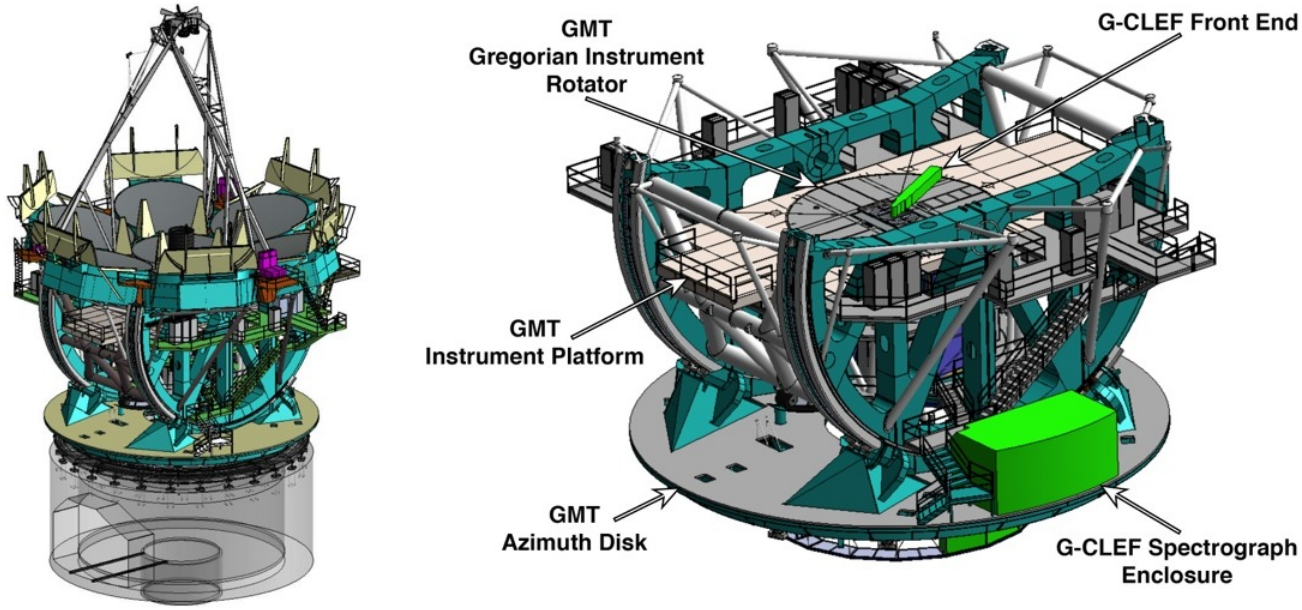


Figure 1: G-CLEF as deployed on the GMT. Left panel is to orient the reader to overall layout of the GMT. The right panel shows the location of the spectrograph thermal enclosure on the azimuth platform and the placement of fold and relay optics ("Front End") on the Gregorian instrument rotator. The optical fiber feed is hidden behind the telescope "C" ring. The fold/relay optics are not shown clocked to their operational azimuth, which is also hidden by the "C" ring.

## 2. SCIENCE AND INSTRUMENT REQUIREMENTS

G-CLEF is designed to be general purpose instrument. The science cases that define the performance of G-CLEF and form the science drivers for G-CLEF have been discussed in a earlier publication[2]. However, several recent scientific developments have increased the need for a high-resolution optical band echelle spectrograph on a telescope with the largest available aperture. These are:

- The discovery of a star so metal poor that no existing facility can measure its iron content, i.e. the strongest available iron absorption lines around 3500 to 3900A in the stellar spectrum are so weak that they are undetectable with existing apertures and instruments.[7]
- The advancement in techniques for measuring molecular features in exoplanet atmosphere spectra from ground based facilities, potentially enabling the detection of biomarkers in transmission during exoplanet transit;[8,9]
- The selection of the Transiting Exoplanet Survey Satellite (TESS) for launch by NASA which will produce an all-sky catalogue of bright exoplanetary systems amenable to detailed study.[10]

In the following sections we supply some information concerning G-CLEF's capability to open up new discovery space in these areas.

### 2.1 Characterization of Metal Poor Stars

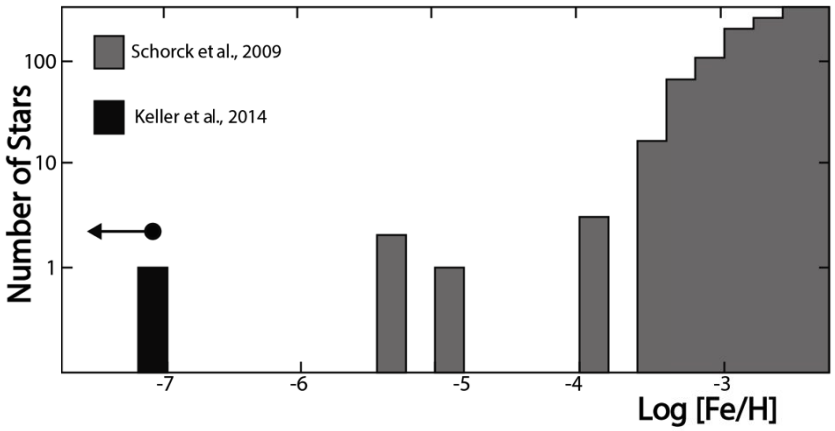


Figure 2: Histogram of the census of the most metal poor stars known. Bars in grey are from Hamburg/ESO Survey[11]. Black bar is the result of Keller et al.[7] which is an upper limit.

Metal poor stars in the local Universe (specifically the Milky Way halo) are the present-day fossils of the earliest phase of star and galaxy formation soon after the Big Bang. In their atmospheres, they preserve the chemical composition of their birth gas cloud which enables reconstruction of the first heavy element enrichment events by massive supernova that first lit up the universe. Additionally, abundance distributions of these elements as observed in the metal-poor stars today yield valuable information about the nature (e.g. mass, explosion energy) of these very first stars and in what environments were formed. This field is often referred to as near-field cosmology. Consequently, there have been extensive efforts focused on systematically finding the most metal-poor stars in the Milky Way and its dwarf satellite galaxies over the last two decades. Figure 2 shows the metallicity distribution function[11] of metal-poor halo stars. The dearth of stars at the lowest iron metallicities, which are the most valuable tracers of the first stars as stars with [Fe/H]<−4, is believed to be representative of the second or third generation of stars that have formed in the universe.

The most metal poor star known until recently has depletions of iron to hydrogen of $10^{-5.4}$ compared to solar abundances[12]. The recent discovery of a star[7] (SMSS J031300.36-670839.3) with a [Fe/H] ratio of <−7.1 (corresponding to $10^{-7.1}$ of the solar iron abundance) has presented a new challenge in the field. Besides being a second generation star to have formed in the universe, no iron lines (in the 3500-3800A region) were detectable in an R~35,000, S/N~120, spectrum after an exposure time of 13 hours. The star has proved too faint and too metal-poor for currently available instrumentation and telescopes to measure these features. Only magnesium and calcium could be measured since other elements have even weaker absorption lines than iron, leaving the abundance signature of this important fossil star largely unexplored.

Measurement of the equivalent width of iron and other elements that will make it possible to determine the chemical abundance signature of SMSS J031300.36-670839.3, including its iron metallicity, precisely requires high resolution spectroscopic capability on one of the extremely large telescopes (ELTs) with good blue sensitivity down to 3500Å.

### 2.2 Weighing Planets in the TESS Catalogue

The TESS mission has been selected for launch in the most recent NASA Small Explorer competition. TESS will launch early 2018, and produce an all-sky survey of bright nearby transiting exoplanetary systems. Because these systems transit, their orbital geometry is well known, and thus it is possible to measure the density of the exoplanets. The transiting geometry of the orbit also makes it possible to detect the atmospheres of exoplanets and determine their molecular composition.

The TESS magnitude range will extend to a faintness of 12$^{th}$ magnitude, overlapping that of the Kepler mission in a band of magnitudes between 10$^{th}$ and 12$^{th}$ magnitude. The Kepler survey was limited to a 100 square degree region of the Northern sky and discovered over 3000 transiting exoplanet candidates. A comparison of TESS, Kepler and ground-based transit survey yields appears in Figure 3.

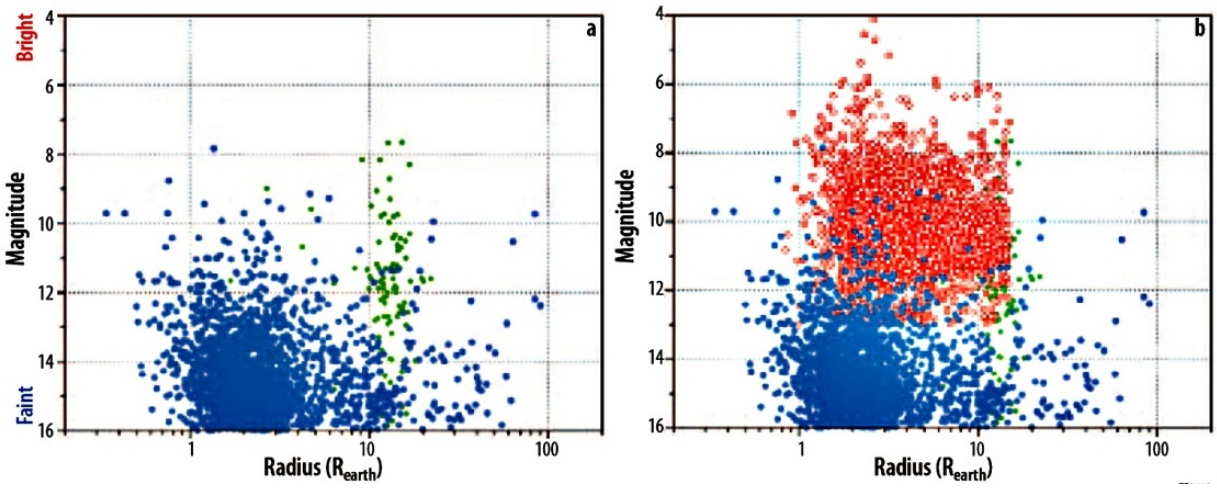


Figure 3: Comparison of brightness of Kepler discoveries plotted in blue, ground-based transit surveys in green and the expected TESS yield in red - (from the TESS Concept Study Report).

A key feature of the TESS catalogue is the brightness of the transiting systems it will discover. At present detailed characterization of exoplanets and their atmospheres is restricted to a very small number of the brightest known exoplanet systems. By discovering a large sample of bright exoplanetary systems, TESS will provide the astrophysics community with a fair sample of objects with which to explore exoplanet bulk properties, exoplanet atmospheres and the properties of planetary systems in general. As an example, TESS is expected to discover 300 or more transiting Earths and Super-Earths.

In Table 1, we compare the detectability of Solar System constituents orbiting stars of various masses. We characterize the detectability of these various systems as 1) within current technical capabilities with existing telescopes and instruments, 2) plausibly achievable with existing telescopes by the time of G-CLEF first light, 3) achievable with specified G-CLEF performance and 4) achievable with goal G-CLEF performance. It is to be noted that except for extremely low mass stellar masses, “exo-Earths” are only detectable with G-CLEF. If G-CLEF meets goal performance, there is the possibility that G-CLEF might detect Mars-mass exoplanets orbiting M-type stars.

While the peak of the spectral energy distribution of M-stars is in the near infrared, it has been shown that the best information content for the measurement of M-star velocities is in 7000−9000Å passband (see Figure 4). For this reason, PRV observations of stars less massive than A-stars require high throughput in the entire 3900−9000Å passband.

Table 1: Reflex velocities for a range of planets masses orbiting solar and M dwarf stars. Currently achievable radial velocity precision is coded in light beige. Extrapolation to the era of G-CLEF first light is highlighted in dark beige/red. G-CLEF specification precision is coded in green and goal precision is indicated in yellow.

| Planet | a (AU) | Required Reflex Velocity Sensitivity (m/sec) | | | | |
|---|---|---|---|---|---|---|
| | | G2V | M0V | M2V | M4V | M6V |
| Jupiter (318 $M_{Earth}$) | 0.1 | 89.8 | 116 | 136 | 201 | 284 |
| Jupiter (318$M_{Earth}$) | 1.0 | 28.4 | 36.7 | 42.9 | 63.6 | 89.9 |
| Jupiter (318 $M_{Earth}$) | 5.0 | 12.7 | 16.4 | 19.1 | 28.4 | 40.2 |
| Neptune (17 $M_{Earth}$) | 0.1 | 4.8 | 6.2 | 7.2 | 10.8 | 15.2 |
| Neptune (17 $M_{Earth}$) | 1.0 | 1.5 | 2.0 | 2.3 | 3.4 | 4.8 |
| Super Earth (5 $M_{Earth}$) | 0.1 | 1.4 | 1.8 | 2.1 | 3.1 | 4.4 |
| Super Earth (5 $M_{Earth}$) | 1.0 | 0.45 | 0.57 | 0.67 | 1.0 | 1.4 |
| Earth | 0.1 | 0.28 | 0.37 | 0.43 | 0.68 | 0.89 |
| Earth | 1.0 | 0.09 | 0.12 | 0.13 | 0.20 | 0.28 |
| Mars (0.11 $M_{Earth}$) | 0.1 | 0.03 | 0.04 | 0.05 | 0. 07 | 0.09 |
| Mars (0.11 $M_{Earth}$) | 1.0 | 0.009 | 0.012 | 0.014 | 0.021 | 0.030 |

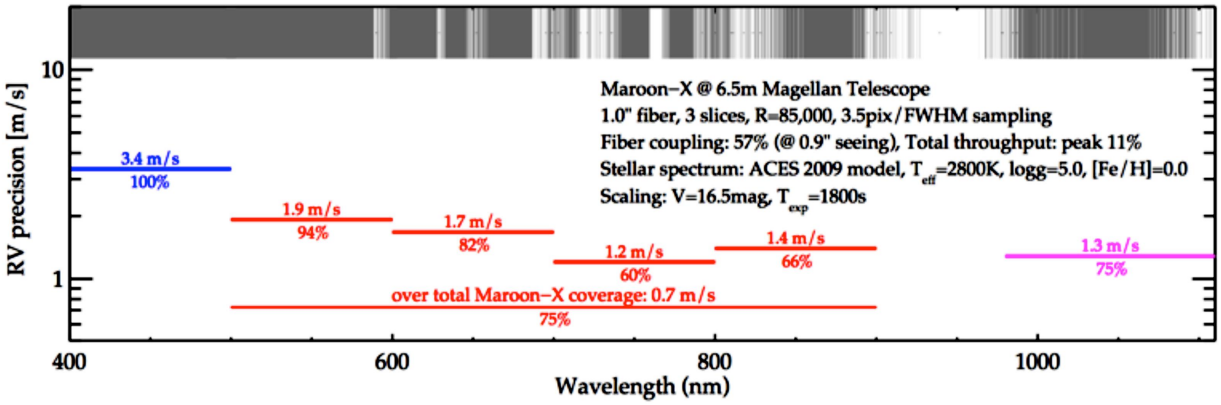


Figure 4: Radial velocity precision expected of a red-sensitive PRV spectrograph on the 6.5m Magellan telescope. The top band shows the telluric atmospheric transmission in reverse. The achievable radial velocity for different passbands is indicated below for an M5 dwarf. Percentages indicates the fraction of the bandwidth that is usable for RV measurements in the passband indicated by the horizontal bars. It can be seen that even though there is considerable absorption in the band near 7500Å, it is the best region for PRV measurement for this star (Bean, 2013)[13].

### 2.3 Search for O2 in the Transmission Spectra of Exoplanets

An important potential indicator of exoplanetary bioactivity is the presence of $O_2$ in exoplanet atmospheres. As several authors have pointed out[8,9], A-band of absorption features between 7600 and 7700Å (see Figure 5) are particularly useful spectral feature to search for during exoplanet transits.

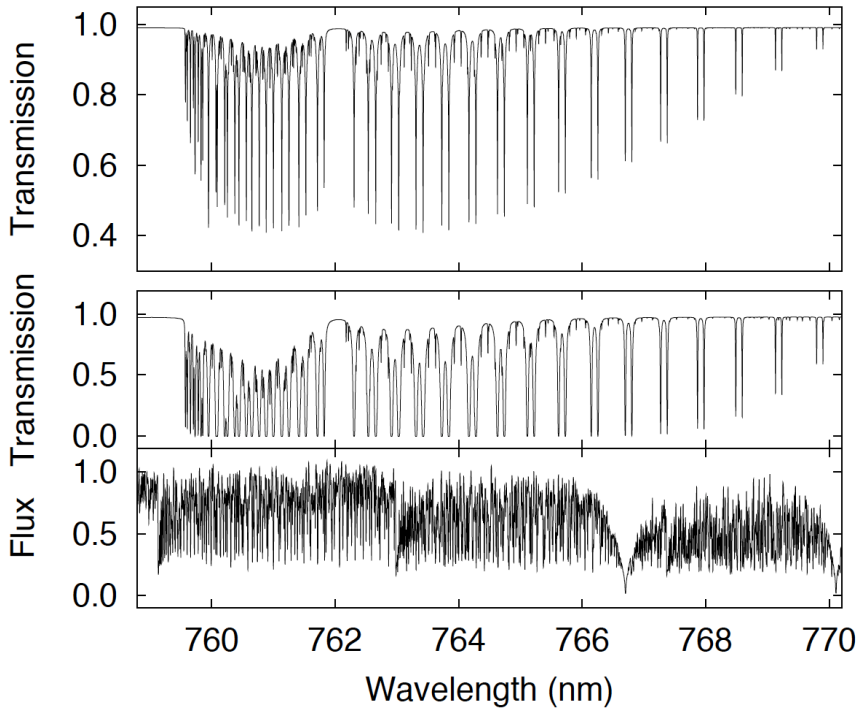


Figure 5: Top panel: transmission spectrum of the atmosphere of an Earth-like planet around 7600Å. Middle panel: telluric spectrum of our atmosphere for a zenith distance of 30° (airmass Z = 1.3). Bottom: PHOENIX model spectrum of an M4V star with a surface temperature of T = 3000 K, log g = 4.5 dex and solar abundance. All spectra are shown at a spectral resolution of R = 100,000 (from Rodler & Lopez-Morales, 2013)[9].

While telluric foreground absorption feature would seem to constitute a insuperable impediment to detecting exoplanetary $O_2$, the features are quite narrow and quite modest relative line of sight velocities between the Earth and an exoplanet are sufficient to Doppler shift the exoplanet feature out from under the telluric absorption, and the exoplanet signal become detectable if observed at high enough resolution ($R \gtrsim 100{,}000$).

Table 2: Simulations of G-CLEF performance on the GMT for a 3σ detection of $O_2$ in the atmospheres of exoplanets in the habitable zone as a function of stellar type. (from Rodler & Lopez-Morales, 2013)[9]. The "obs. time" is the total time required to make the observations. Since the G2V through M3V examples will be quite bright, observations will be extremely short to avoid saturation of the the detector, so readout time of the detector will reduce observational "Duty Cycle".

| Type | Obs. Time (h) | Duty Cycle | Transits | Time (years) |
|---|---|---|---|---|
| G2V | 470 | 0.18 | 37 | 37 |
| M1V | 133 | 0.86 | 33 | 35 |
| M2V | 133 | 0.91 | 40 | 31 |
| M3V | 130 | 0.94 | 44 | 28 |
| M4V | 70 | 0.98 | 34 | 14 |
| M5V | 79 | 0.98 | 53 | 12 |
| M6V | 75 | 0.98 | 68 | 10 |
| M7V | 61 | 0.98 | 78 | 8 |
| M8V | 69 | 0.98 | 100 | 8 |
| M9V | 67 | 0.98 | 154 | 7 |

Results of detailed analyses summarized in Table 2 suggest that while fairly long observational campaigns may be required with the GMT to detect $O_2$ in exoplanet atmospheres orbiting around G, K and early-type M stars; later-type M stars may be good targets for the search for bioactivity.

## 3. SYSTEM ENGINEERING AND DESIGN

G-CLEF is a fiber-fed, cross-dispersed echelle spectrograph. Its working passband is 3500Å−1 μm. The required blue wavelength limit is set by the requirement to observe a complex of iron lines for abundance measurements, especially studies of metal poor stars. These lines are slightly redder than 3500Å. The red limit of G-CLEF is determined by cosmology programs and PRV searches for low-mass planets orbiting M-stars (see Figure 4). The decision to fiber-feed G-CLEF was to maximize the wavelength-scale stability of the spectrograph for PRV observations. The fiber run has been made as short as possible to minimize the attenuation of the blue end by the optical fiber. A decision was taken early in the design process that a two camera design was necessary to deliver good imaging performance with high throughput.

Different science programs have different resolution requirements. Since an optical fiber is a fixed format slit, we feed the spectrograph with four distinct fiber feed system. We also have an interface to a multi-object system being developed by the Australian Astronomical Observatory – MANy-Instrument FibEr positioning SysTem (MANIFEST). These are enumerated in Table 3.

Table 3: Operation modes of G-CLEF – Precision Radial Velocity (PRV), Non-Scrambled, Precision Radial Velocity (NS-PRV), Medium Throughtput (MT), High Throughput (HT), and Multi-Object Spectroscopy (MOS).

| Fiber Mode | Resolution | Fiber Diam. (μm)/arcsec | Mode Scrambled ? | Comments |
|---|---|---|---|---|
| PRV | 105,000 | 100/0.97 | Yes | Precision Radial Velocity, Pupil Sliced x 7 |
| NS-PRV | 105,000 | 100/0.97 | No | Pupil Sliced × 7 |
| MT | 35,000 | 300/0.79 | No | |
| HT | 19,000 | 450/1.2 | No | |
| MOS | 35,000 | 300/0.79 | No | Through MANIFEST, Multiplex = 40 |

**PRV Modes:** RV measurement is optimized when the absorption features of F,G & K stars are fully resolved. This is achieved with a resolution of R >100,000 for all latest K-type stars[14]. Since it seemed impractical to design a buildable spectrograph with the requisite beam size to deliver resolution this high for a 25.4 m aperture, we chose to pupil-slice the GMT aperture into seven 8.4 m apertures. For ultimate RV precision it is necessary to mode scramble the optical fibers, however this cause a ~20% loss of system throughput. For observations that require this highest resolution, but do not require ultimate RV precision, we offer a second non-scrambled PRV mode (NS-PRV). A stand-alone contribution to these proceeding describes a system engineering approach to developing error budget for radial velocity precision and the reader is encouraged to look there for more details[5].

**MT Mode:** Detailed stellar abundance studies require resolution in the 35,000−40,000 range, which is achieved with a 300 μm diameter optical fiber which is 0.79 arcsec seeing, i.e. the median seeing at Las Campanas.

**HT Mode:** For programs where signal-to-noise, hence throughput, is paramount, a 450 μm fiber is 1.2 arcsec on the sky provide a high throughput mode with resolution of 20,000.

**MOS Mode:** The MANIFEST program is not yet at the same level of development as G-CLEF, since MANIFEST will not be delivered at first light, and a final decision has not yet been taken on the resolution, however the current baseline is for R~35,000 and a multiplex of 40 simultaneous fibers.

### 3.1 Spectrograph Systems Engineering

The system engineering of G-CLEF is focused on maximizing efficiency over the entire G-CLEF passband, while maintaining PRV capability. Since G-CLEF is a high-resolution spectrograph for an unprecedentedly large aperture, a rigorous systems approach to cost and risk is required for a project of this scale. To maximize throughput, we have sought to minimize the number of vacuum-glass interfaces. We have also split the camera into blue and red channels to optimize coatings, substrates and detectors for narrower, specific passbands.

We have also minimized the length of the fiber run between the telescope interface and the spectrograph, which might compromise throughput at bluer wavelengths if the run were too long. Before selecting a relayed fiber feed we conducted a trade study to compare a fiber feed, a Coudé feed and a hybrid feed. We found that while the complexity of

a Coudé or hybrid feed was significantly higher, increasing cost and risk, however they did not offer markedly better throughput, even at the blue end of the passband.

The requirement for PRV capability has required us to develop an extremely stable spectrograph design, with superb thermal control to minimize time-variable thermal gradients in the spectrographs structure, deployment at a gravity-invariant location on the telescope and stabilization of the ambient pressure of the spectrograph environment. We have chosen to adopt the technique employed by the HARPS[15] and HARPS-N instrument teams and to enclose the spectrograph in vacuum and thus simultaneously stabilize the pressure and minimize parasitic transfer of heat by convection or conduction. A rigorous PRV error budget has been developed to allocate RV error terms to various subsystems and processes, and thus meet operational requirements[5].

A very important issue is that of heat management, so that G-CLEF maintains the spectrograph at a fixed temperature year-round, but does not leak excessive heat into the dome which would compromise dome seeing.

### 3.2 Telescope Interface/Front End Systems Engineering

The telescope interface, or "front end" serves several important function, including:

- Flexure control;
- Telescope beam relay;
- Atmospheric dispersion compensation;
- Fiber mode selection;
- Calibration light injection;
- Shutter function.

The capability to exploit the adaptive optics system is also included in the requirements for the front end. A function diagram of the G-CLEF front end is shown in Figure 6.

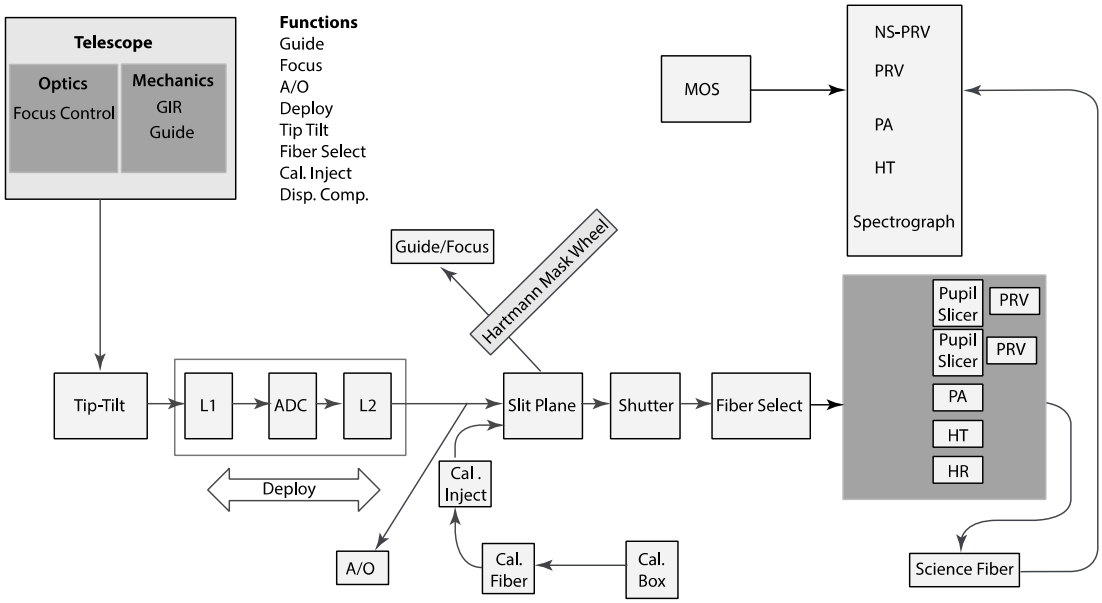


Figure 6: Front End System Diagram

**Flexure Control:** The GMT will be exquisitely guided and focused by the Acquisition, Guide and Wavefront System (AGWS)[16]. However, the optical paths to the AGWS and the G-CLEF optical fiber are not the same. Differential flexure between the two optical trains must be compensated. The G-CLEF flexure control system is then a localized guide and focus system. Because flexure will be very slow, the control loop has a very long time constant. A deployable tip-tilt

mirror, which also folds the telescope beam toward the G-CLEF fiber inputs will compensate flexure. A Hartmann mask in -the guide camera arm will measure focus and send focus updates directly to the telescope control system. For brighter objects, guide will be measured using the light that overflows the fiber slit, i.e. guiding on the science object itself. For fainter objects, offset-guiding will be implemented. Since the front end itself is not derotated and the GMT is an alt-az telescope, a fairly detailed investigation was made of the necessity of a guider derotation mechanism. We determined that except for guiding within ~3° of zenith-pointing, guiding in V+R+I on a 25$^{th}$ V magnitude offset guide object at the edge of the guide field, there was adequate signal-to-noise to guide without rotation. Within 3° of zenith, flexure will be negligible and will not require compensation. The guide field is square, 1.5' on a side, and the probability of finding a guide object in that field in the sparsest fields at the galactic polar cap is greater than 99%.

**Telescope Beam Relay:** The Gregorian focus of the GMT, when folded to the G-CLEF fiber inputs, is quite close to the optical axis of the telescope itself, on a rotating platform called the Gregorian Instrument Rotator (GIR). The fibers themselves must be mounted to a non-rotating section of the telescope on the Instrument Platform (IP). It is desirable to locate the G-CLEF fiber inputs as close to the edge of the IP so as to minimize fiber length and maximize throughput at blue wavelengths. A system of relay optics, described later in this paper, is needed to relay the beam from the telescope focus to the fiber inputs.

**Atmospheric Dispersion Compensation (ADC):** All GMT instruments are required to operate efficiently to a zenith distance of 60°. Circular fiber slit inputs will suffer wavelength dependent losses at even modest air masses if atmospheric dispersion is not compensated. For this reason an atmospheric dispersion compensator is an integral part of the front end design.

### 3.3 Calibration System

The calibration system is modeled extensively on that developed for HARPS[15] and HARPS-N. The calibration light sources are located remotely from either the spectrograph and front end. Calibration light is conveyed to the front end by optical fibers that feed calibration light into the input of the science optical fibers at the front end. This system can inject any of the light sources into any of the fibers, and the exit pupil and focal ratio of the telescope are simulated with preoptics that are integral to the injection system.

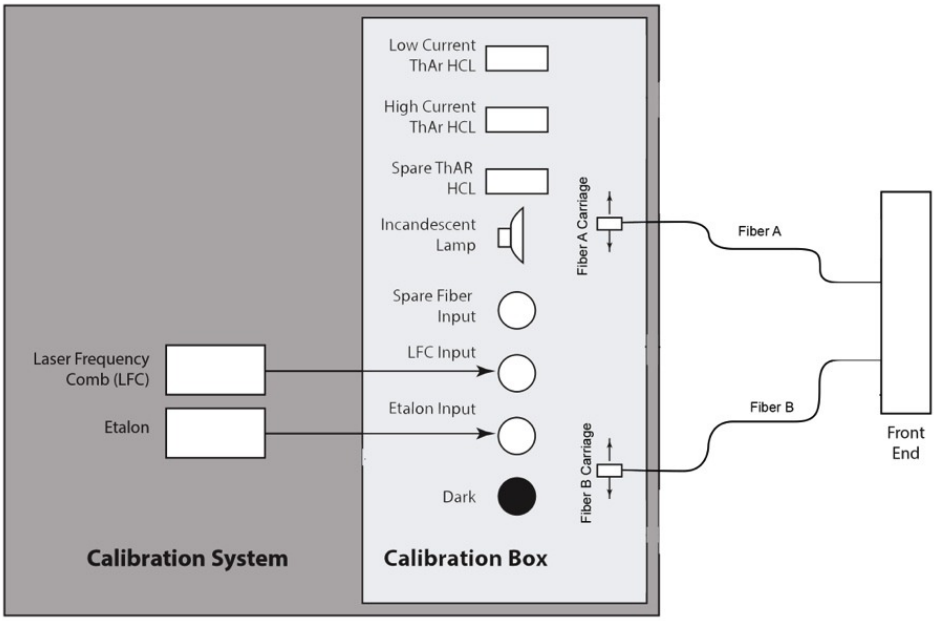


Figure 7: System diagram of the calibration light source system.

The calibration system will contain several light sources and the light source is selected by linear actuation of the calibration fiber input within the calibration box (see Figure 7). We, in collaboration with other instrument teams, are experimenting with a number of alternative calibrators that have the potential to enable more precise and accurate calibrations, especially laser frequency combs and ultrastabilized etalons[17].

# 4. OPTICAL DESIGN

## 4.1 SPECTROGRAPH OPTICAL DESIGN

The optical design of the G-CLEF spectrograph is an asymmetric white pupil design.[18,19]. A full discussion of the optical design appears in another contribution to this proceedings, so here we discuss several innovative features of the spectrograph optical design.

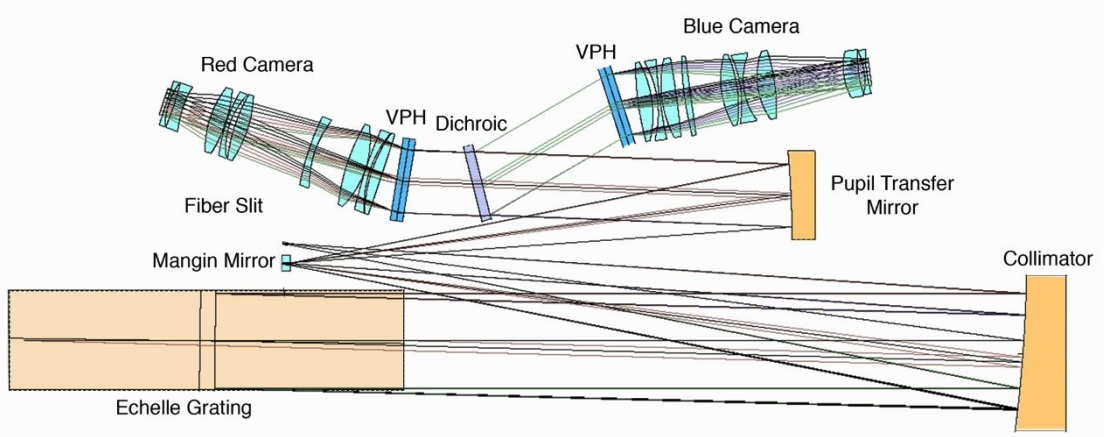


Figure 8: Optical layout of the G-CLEF spectrograph.

The optical layout of the G-CLEF spectrograph is shown in Figure 8. There are no moving parts in G-CLEF which might dissipate heat so as to maximize thermal stability and hence wavelength scale stability for PRV observations. The focal ratio of the beam is immediately adjusted from the f/3 beam emergent from the fibers to f/8. The spectrograph beam is 300 mm in diameter in the foresection of the optical train. The echelle spectrograph is a triple mosaic of 300 mm × 400 mm grating facets that will be replicated by Richardson Gratings. The collimator is an off-axis paraboloid.

The beam is folded by a toroidal Mangin mirror, which makes the overall layout more compact and compensates anamorphic field curvature that is intrinsic to this type of spectrograph design. The field curvature has been compensated in other white pupil designs with a cylindrical lens very close to the focal plane. However the correction is not as good as that achieved with a Mangin mirror near the internal focus of the optical train. Another alternative is to curve the focal plane itself. While this gives the best correction, an in-depth canvass of potential vendors for a curved focal plane revealed that the development costs for a curved focal plane would be prohibitively expensive. The use of a Mangin mirror is discussed in another presentation in these proceeedings[3].

The beam is then recollimated and demagnified with an ellipsoidal pupil transfer mirror and split by a dichroic. The demagnification reduces the beam size to 200 mm, reducing the requirements for large diameter substrates for the camera lenses. The beam is split into red and blue channels with a dichroic at 5400Å. Cross dispersion is effected with volume phase holographic (VPH) gratings. Each camera has 9 spherical elements. The 8$^{th}$ element of each camera forms the vacuum window of the CCD cryostat. The CCD we have baselined is 6k × 6k, 15 μm pixels device.

The performance and detailed optical design can be found in Furesz, et al[3].

## 4.2 TELESCOPE INTERFACE OPTICAL DESIGN

The telescope interface, or G-CLEF front end, is mounted just below the primary mirror on the GIR and IP. The GIR typically is used to derotate the sky, however the use of a fiber feed for G-CLEF requires the GIR not move during G-CLEF operations. After detailed study, it was determined that no derotation was necessary for G-CLEF observations. The relay system (see Figure 9) consists of two triplets, consisting of Ohara i-Line glasses and calcium fluoride to maintain high transmission to 3500Å. The ADC is also fabricated out of i-Line glass, and consists of two pairs of planar zero deviation, counter-rotating prisms.

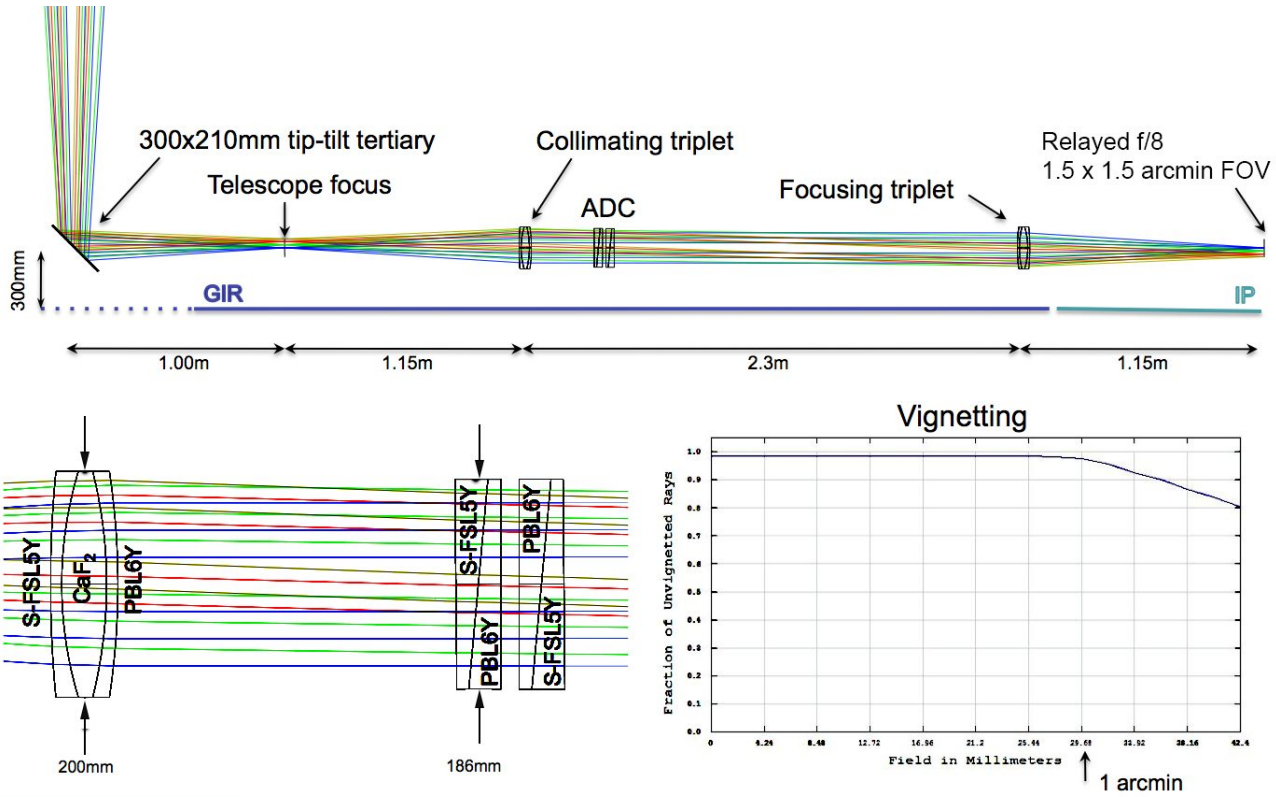


Figure 9: Telescope interface tip-tilt, relay optics and atmospheric dispersion compensator at CoDR. All optics are on the Gregorian Instrument Rotator (GIR), which is fixed during G-CLEF observations. The fiber interface is on the fixed instrument platform. Vignetting in the CoDR design is minimal.

The science fibers are embedded in a mirror tilted at 10° with respect to the relayed beam to reflect light to the flexure compensating camera. This camera is required to measure non-common mode focus and guide errors between the G-CLEF arm and the AGWS arms of the GMT. The optical design is required to have a pupil where a Hartmann mask can be inserted to update focus at a regular cadence. Since flexure induced focus and guide error will be slow, there is adequate time to switch between guide and focus measurements. The design and optical performance of the camera are shown in Figure 10.

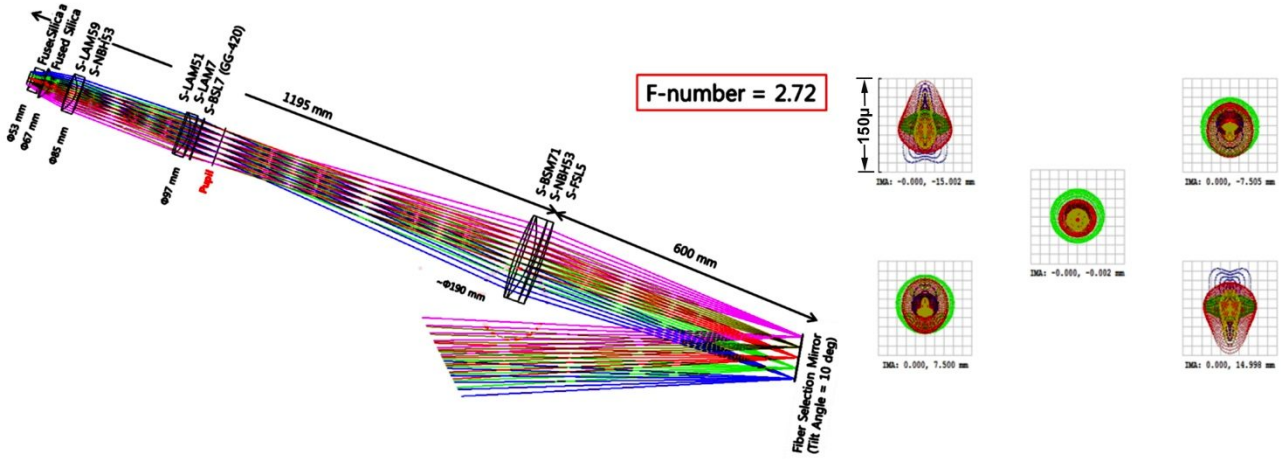


Figure 10: Flexure control (guide and focus) camera optical design and spot diagrams. The plate scale at f/2.72 is 340 µm/arcsec.

## 5. MECHANICAL DESIGN

The mechanical design of the G-CLEF spectrograph at CoDR is shown in Figure 11. This mechanical design is the subject of paper elsewhere in these proceedings, so we only point out some of the highlights of the design[4]. The fiber slit holds all the fibers required to support the various observing modes in fixed format. Different modes are selected by a shutter at the input end of the fiber run. The collimator is a mirror that has been significantly apodized to fit within the space envelope of the spectrograph. This is also true of the pupil transfer mirror. When cutting these optics out of their parents, the vertices of the mirrors are not included in the apodized optic.

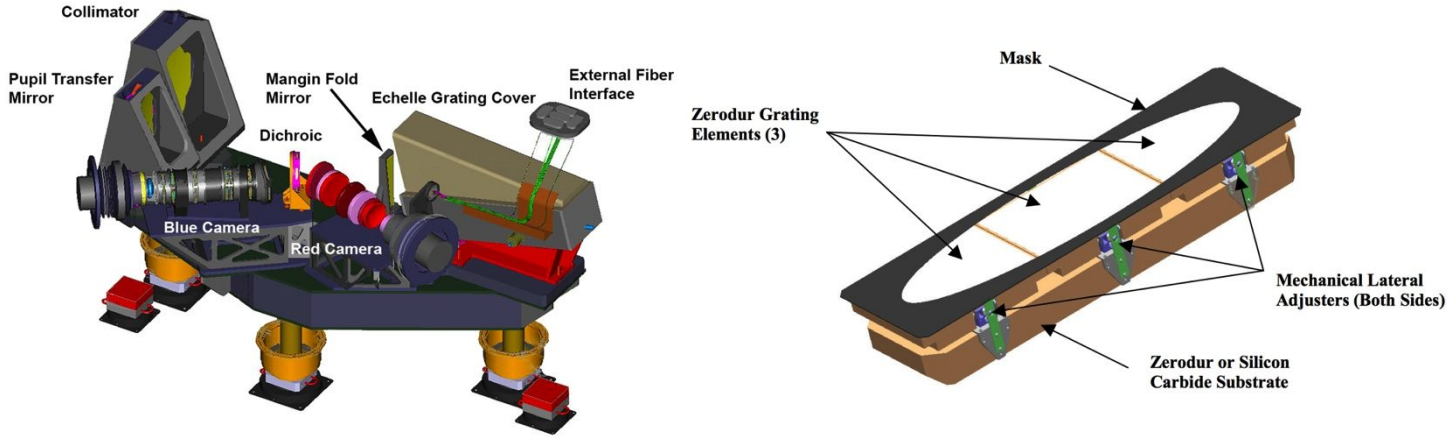


Figure 11: Left panel – a mechanical drawing of the G-CLEF spectrograph at CoDR. Right panel – a concept for mounting the G-CLEF triple mosaic echelle grating based on the KECK HIRES triple mosaic design[20].

All lenses and mirrors are mounted with hard-bonded tangent flexures. The large triple mosaic echelle grating poses a particular challenge, given the size of the grating, as well as the co-alignment precision and stability required for this optic. We investigated the possibility of replicating three rulings onto a single substate – Richardson Gratings has manufactured double replications for other instruments – however the development costs were prohibitively high. We also considered bonding three individual gratings to a monolithic substrate, but a risk analysis of the bonding process was considered to carry unacceptable risk and/or cost. Our baseline is a metering structure shown in Figure 11, in which the piston and tilt of each facet is set with Zerodur shims and rotation of the facet is set with precision adjusters.

The mechanical design of the front end is shown in Figure 12. The tertiary, collimating relay lens and ADC are deployed so as to intercept the telescope beam during G-CLEF observations and retracted when other instruments are in use. These optics, along with the focusing relay lens, are mounted on the GIR, which rotates to select instruments for observation and to derotate field rotation. The flexure compensation camera, fiber mode selector, shutter and interface to the science and calibration system are grouped together on the IP. This minimizes the length of the science optical fiber run, and maximizes blue throughput. This design was developed for CoDR. A design that includes a refined flexure control capability and an interface to the AO system is now in progress.

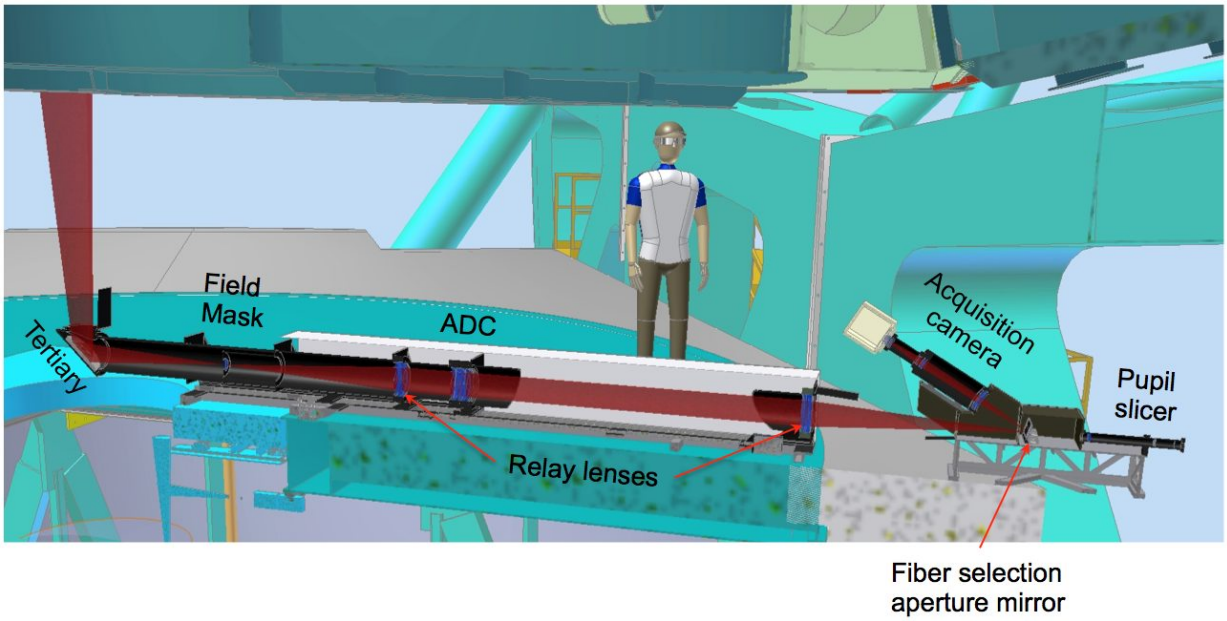


Figure 12: The mechanical layout of the front end structure.

## 6. EFFICIENCY PREDICTION

The most important figure of merit for any astronomical instrument is its efficiency, i.e. how successfully it exploits the aperture of a given telescope. Given that the GMT may, for some time, be the largest optical band telescope in the world, it is crucial that G-CLEF not squander a unique asset. We have calculated the expected throughput of G-CLEF on the GMT. All losses have been included, i.e atmosphere losses, telescope reflectivity, slit losses and losses in the fiber system and spectrograph. This has been calculated for zenith pointing and median (0.79 arcsec) seeing. The seeing disk is modeled as a Gaussian profile. Reflectivity and transmission of the various coatings are taken as that fresh from the vendor. While there will be some erosion of throughput due to wear, contamination and dirt, the bulk of the optical train is vacuum enclosed, so our prediction is not overly optimistic.

The results of this calculation are presented in Figure 13. The discontinuity at 5400Å is due to the cross-over between the red and blue cameras.

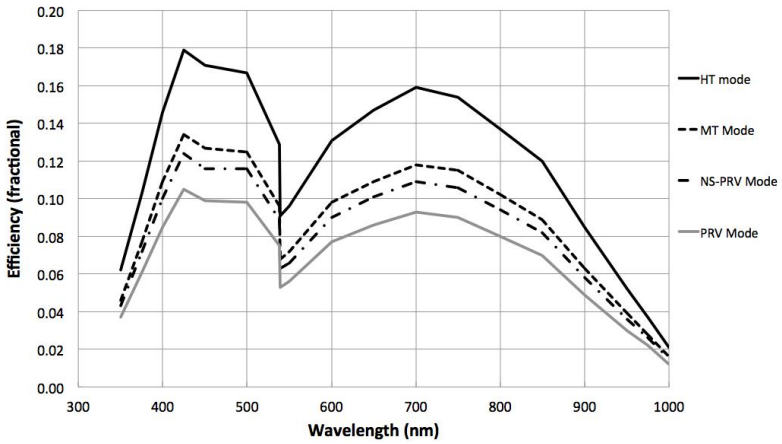


Figure 13: Predicted efficiency of G-CLEF in various observing modes

### 6.1 The Impact of Adaptive Optics

Shortly after first light, the GMT will have full AO capability enabled by adaptive secondary mirrors[21]. While conventional wisdom is that AO offers little improvement in performance in the optical pass band, we modeled the encircled energy and encircled energy stability as a function of correction strategy with the GMT system[22]. The results of this modeling effort are summarized in Table 4 and Table 5, which compare natural seeing, tip-tilt correction, ground layer AO (GLAO) and high order AO. Rather remarkably, each enhancement in wavefront correction improves both the concentration and the stability of the point spread function to a blue limit of 4000Å. High order AO improves throughput by 60−75% and the stability of the PSF increases by a factor of 5−10 over natural seeing, with the greatest improvement at the red end of the G-CLEF passband. PSF stability translates into near and far field stability within the spectrograph and will contribute materially to improving wavelength scale stability, hence RV precision. A test of this modeling is scheduled for Fall 2014 using the Magellan AO system and laboratory experiments using atmospheric turbulence simulators.

Table 4: Encircled energy in 0.7 arcsec diameter as a function of wavelength and correction method.

| Wavelength | 4400Å | 5500Å | 6400Å | 7900Å |
|---|---|---|---|---|
| Natural Seeing | 0.39 | 0.41 | 0.42 | 0.45 |
| Tip-Tilt Correction | 0.49 | 0.52 | 0.54 | 0.57 |
| GLAO | 0.52 | 0.55 | 0.57 | 0.60 |
| High Order AO | 0.68 | 0.71 | 0.73 | 0.75 |

Table 5: Variation (RMS) of encircled energy in 0.7 arcsec diameter in 10 msec integrations.

| Wavelength | 4400Å | 5500Å | 6400Å | 7900Å |
|---|---|---|---|---|
| Natural Seeing | 0.0561 | 0.0617 | 0.0660 | 0.0725 |
| Tip-Tilt Correction | 0.0229 | 0.0251 | 0.0266 | 0.0287 |
| GLAO | 0.0281 | 0.0308 | 0.0327 | 0.0352 |
| High Order AO | 0.0095 | 0.0085 | 0.0077 | 0.0074 |

## 7. SCHEDULE

The construction phase of the GMT is expected to commence Jul 2014. PDR for G-CLEF is scheduled for March 2015.

Delivery of G-CLEF to the GMT is planned for 2019 and science operations will start in 2020. At first light, the GMT will have four of its seven primary mirrors and will operate with fast steering secondaries rather than a fully adaptive secondary system. The full seven primaries and adaptive secondaries will be delivered in the 2020 – 2022 time frame.

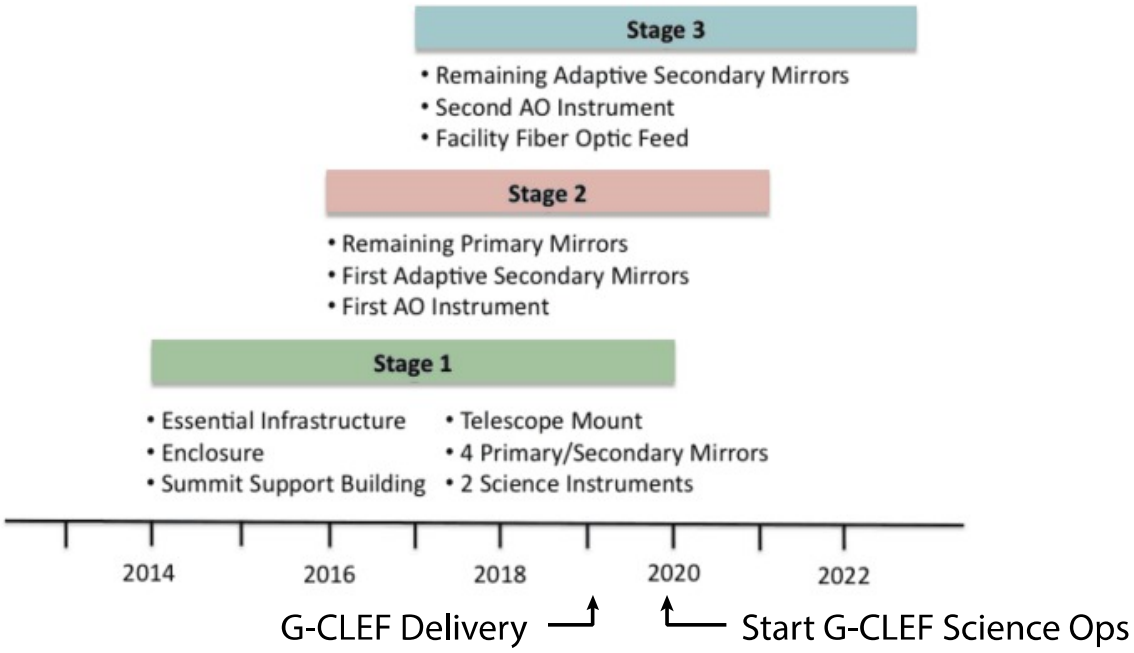


Figure 14: Schedule for the completion of the G-CLEF and the GMT

## REFERENCES


[1] Bernstein, R.A., Johns, M., McCarthy, P., Raybould, K., Bigelow, B. Bouchez, A., Filgueira, J., Jacoby, G., Sawyer, D., Sheehan, M.,"Overview and status of the Giant Magellan Telescope", Proc. SPIE, 9147 (These proceedings), 9145-47, (2014).

[2] Szentgyorgyi, A., et al., "The GMT-CfA, Carnegie, Catolica, Chicago Large Earth Finder (G-CLEF): a general purpose optical echelle spectrograph for the GMT with precision radial velocity capability", Proc. SPIE, (2012).

[3] Furesz, G. et al., "The G-CLEF spectrograph optical design: an update to the white pupil echelle configuration", Proc. SPIE, 9147 (These proceedings), 9147-353, (2014).

[4] Mueller, M. et al., "The optomechanical design of the GMT-Consortium Large Earth Finder (G-CLEF)", Proc. SPIE, 9147 (These proceedings), 9147-347, (2104).

[5] Podgorski, W. A., et al., "A novel systems engineering approach to the design of a precision radial velocity spectrograph − the GMT-Consortium Large Earth Finder (G-CLEF)", Proc. SPIE, 9147 (These proceedings), 9147-333, (2014).

[6] Jacoby, G., et al., "The status of the instrument development program for the Giant Magellan Telescope", Proc. SPIE, 9147 (These proceedings), 9147-70, (2014).

[7] Keller, S., Bessell, M.S., Frebel, A., Casey, A.R., Asplund, M., Jacobson, H.R., Lind, K., Norris, J.E., Yong, D., Heber, A., Magic, Z., da Costa, G.S., Schmidt, B.P. and Tisserand, P., "A single low-energy, iron-poor supernova as the source of metals in the star SMSS J0313000.36-670839.3", Nature, 7489, 463, (2014).

[8] Snellen, I.A.G., de Kok, R.J., le Poole, R., Brogi, M. and Birkby, J., "Finding extraterrestrial life using ground-based high-dispersion spectroscopy", ApJ, 764, 182, (2013).

[9] Rodler, F. and Lopez-Morales, M., "Feasibility studies for the detection of $O_2$ in an Earth-like exoplanet", ApJ, 781, 12, (2014).

[10] Ricker, G., "The Transiting Exoplanet Survey Satellite (TESS)", Proc. SPIE, 9147 (These proceedings), 9143-508, (2014).

[11] Schorck, T. et al.,"The stellar content of the Hamburg/ESO survey. V. The metallicity distribution function of the galactic halo.", A&A, 507, 817, (2009).

[12] Frebel, A, et al. "Nucleosynthetic signatures of the first stars", Nature, 434, 871, (2005).

[13] Bean, J., Private communication, (2013)
[14] Bouchy, F., Pepe, F. and Queloz, D., "Fundamental photon noise limit to radial velocity measurements", A & A, 374, 733, (2001).
[15] Lovis, C., et al.,"The exoplanet hunter HARPS: unequalled accuracy and perspectives towards 1 cm $s^{-1}$ precision", Proc. SPIE, 6269, 23L, (2006).
[16] McLeod, B., Bouchez, Filgueira, J., John, M., Norton, T., Ordway, M., Podgorski, W. and Roll, J., "The Giant Magellan Telescope active optics system", Proc. SPIE, 9147 (These proceedings), 9145-64, (2014).
[17] Wildi, F., Chazelas, B. and Pepe, F., "A passive, cost effective solution for the high accuracy wavelength calibration of radial velocity spectrographs.". Proc. SPIE, 84468E, (2012).
[18] Barannne, A. and Duchesne, M."Le spectrographe coude echel.e.c. 152", Proc of ESO/CERN Conference on Auxiliary Instrumentation for Large Telescopes", 241, (1972).
[19] Dekker, H., Delabre, B. and Dodorico, S., "ESO's multimode instrument for the Nasmyth focus of the 3.5 m New Technology Telescope", Proc. SPIE, 627, 339, (1986).
[20] Vogt, S., et al., "HIRES: the high resolution echelle spectrometer on the Keck telescope.", Proc. SPIE, 2198, 362, (1994).
[21] Bouchez, A., "The Giant Magellan telescope adaptive optics program", Proc. SPIE, 9147 (These proceedings), 9148-31, (2014).
[22] van Dam, M., Private communication, (2013).